45. World Development Report, Oxford University Press, New York, p. 300.
46. Subramanian, V., *Water: Quantity – Quality Perspectives in South Asia*, Kingston Int. Publ., Surrey, UK, 2000, p. 256.
47. Singh, B. K., M Phil thesis, Jawaharlal Nehru University, New Delhi, 1983.
48. Singh, B. K. and Subramanian, V., *J. Geol. Soc. India*, 1988, **31**, 579–583.
49. Abbas, N., M Phil thesis, Jawaharlal Nehru University, New Delhi, 1982.
50. Pande, K. S. and Sharma, S. D., *Pollut. Res.*, 1998, **17**, 409–415.
51. Abbi, R., M Sc project report, Jawaharlal Nehru University, New Delhi, 1999.
52. Gupta, L. P. and Subramanian, V., *Environ. Geol.*, 1994, **24**, 235–243.
53. Singh, S. K., M Phil thesis, Jawaharlal Nehru University, New Delhi, 1988.
54. Jha, P. K., M Phil thesis, Jawaharlal Nehru University, New Delhi, 1983.
55. Datta, D. K. and Subramanian, V., *J. Hydrol.*, 1996, **198**, 196–208.
56. Datta, D. K., Gupta, L. P. and Subramanian, V., *Environ. Geol.*, 2000, **39**, 1163–1168.
57. Mahanta, C., M Phil thesis, Jawaharlal Nehru University, New Delhi, 1990.
58. Sahu, D. K., M Sc project report, Jawaharlal Nehru University, New Delhi, 1998.
59. Chakrapani, G. J., M Phil thesis, Jawaharlal Nehru University, New Delhi, 1988.
60. Chakrapani, G. J. and Subramanian, V., *Chem. Geol.*, 1990, **81**, 241–253.
61. Aravinda, H. B., Manjappa, S. and Puttaiah, E. T., *Pollut. Res.*, 1998, **17**, 371–375.
62. Ramesh, R. and Subramanian, V., *J. Hydrol.*, 1988, **103**, 139–155.
63. Kumar, S. P., M Phil thesis, Jawaharlal Nehru University, New Delhi, 1993.
64. Ramanathan, A. L., Vaithiyanathan, P., Subramanian, V. and Das, B. K., *Water Res.*, 1994, **28**, 1585–1593.
65. Bajpayee, S. K., M Phil thesis, Jawaharlal Nehru University, New Delhi, 1998.
66. Niraj, M Sc project report, Jawaharlal Nehru University, New Delhi, 1999.
67. Hasnain, S. I., Subramanian, V. and Dhanpal, K., *J. Hydrol.*, 1989, **106**, 99–108.
68. Subramanian, V., *Estuaries*, 1993, **16**, 453–458.
69. Verma, A., M Sc project report, Jawaharlal Nehru University, New Delhi, 1997.
70. Ramanathan, A. L., Vaithiyanathan, P., Subramanian, V. and Das, B. K., *Estuaries*, 1993, **16**, 459–474.
71. Ramanathan, A. L., Subramanian, V., Ramesh, R., Chidambaram, S. and James, A., *Environ. Geol.*, 1999, **37**, 223–233.
72. Verma, A., M. Phil thesis, Jawaharlal Nehru University, New Delhi, 1999.
73. Ramesh, R., M Phil thesis, Jawaharlal Nehru University, New Delhi, 1983.
74. Ramesh, R. and Subramanian, V., *Indian J. Mar. Sci.*, 1985, **14**, 79–84.
75. Reddy, M. S., M Sc project report, Jawaharlal Nehru University, New Delhi, 1998.
76. Rao, A. S., Rao, P. R. and Rao, N. S., *Indian J. Environ. Health*, 1999, **141**, 300–311.
77. Khare, P., Kulshrestha, U. C., Saxena, A., Kumar, N., Kumari, K. M. and Srivastava, S. S., *Indian J. Environ. Health*, 1996, **38**, 86–94.
78. *Economic and Social Commission for Asia and the Pacific*, Water Resources Series, United Nations, 1995, vol. 74, p. 304.

ACKNOWLEDGEMENT. Data presented in this paper were based on a project funded by Rajiv Gandhi Drinking Water Mission (MRD), DST and MOEF, Government of India.

Received 22 June 2000; revised accepted 30 December 2000

# Large scale Antarctic features captured by multi-frequency scanning microwave radiometer on-board OCEANSAT–1

**N. K. Vyas[†,**], M. K. Dash[†], S. M. Bhandari[†], N. Khare*, A. Mitra* and P. C. Pandey***

[†]Space Applications Centre, Ahmedabad 380 015, India
*National Centre for Antarctic and Ocean Research, Goa 403 804, India

**This paper discusses the features observed over the Antarctic in the passive microwave emission region by the multi-frequency scanning microwave radiometer (MSMR) instrument on-board the Indian remote sensing satellite IRS-P4, now called OCEANSAT–1. Brightness temperature images produced from MSMR show a clear distinction between open water and sea-ice-covered regions. It is also possible to differentiate several levels of ice concentration in the Antarctic Circumpolar Ocean. A number of land features like the Trans-Antarctic Mountain Ranges, part of Gamburtsev sub-glacial mountains, Wilkes and Aurora sub-glacial basins, etc. can be demarcated as well. The consistent quality and regular availability of MSMR data since June 1999 serve as a very useful tool in all-weather day-and-night monitoring of the Antarctic region. MSMR data used in continuation of ESMR, SMMR and SSM/I data, would prove valuable in the study of long-term changes in the polar cryosphere associated with global climate change.**

ANTARCTICA, covering an area of 14 million km$^2$, with an average ice thickness of about 2–3 km, is an important component of the earth's climate system. The sea-ice extent over the Antarctic Circumpolar Ocean varies between 2 and 18 million km$^2$ from summer to winter, strongly influencing the Antarctic Ocean bottom water formation and thus modifying the physical, chemical and biological properties of the world's oceans[1,2].

The polar-ice plays an important role in the global climate system and is potentially a sensitive indicator of the effects of the global change. Both the land and the

**For correspondence. (e-mail: nkv15@yahoo.com)

sea ice, modify the energy balance at the earth's surface. This modulates, through a feedback mechanism, the atmospheric and oceanic circulation patterns and finally affects the weather and the climate. Real-time information on the distribution of sea-ice in the polar regions also helps in optimizing ship navigation in terms of savings in time and fuel, as well as in terms of safety. Continuous monitoring of the state of the polar cryosphere is therefore of paramount importance. Logistic difficulties in making *in situ* measurements in remote inhospitable polar regions make remote sensing from space the most appropriate alternative for large-scale data collection, away from the relatively small number of established ground stations. In fact, over the last two decades, space-based remote sensing has provided vast amount of information about the environmental conditions in the Arctic and the Antarctic[2]. In particular, remote sensing in the microwave band has helped in monitoring polar regions irrespective of illumination conditions and cloud cover. Sea-ice studies have been carried out since 1973 using Nimbus-5 electrically scanning microwave radiometer (ESMR)[1], Nimbus-7 scanning multi-channel microwave radiometer (SMMR)[2] and the defence meteorological satellite programme (DMSP) special sensor microwave imager (SSM/I) data[3]. Recently, an attempt has been made to use SSM/I data to delineate snow-cover changes over the Antarctic during the depletion phase associated with the onset of Antarctic summer[4]. Active microwave imaging and non imaging sensors, e.g. radar altimeters, radar scatterometers and synthetic aperture radars have also been used to study many features of Antarctic ice with high spatial resolution[5].

On 26 May 1999, India launched its Indian Remote Sensing satellite, IRS-P4, christened OCEANSAT–1, in a near polar sun-synchronous orbit at an altitude of 720 km with the local time of equatorial crossing in the descending node at 12:00 h. It contains two payloads, the ocean colour monitor (OCM) and the multi-frequency scanning microwave radiometer (MSMR). MSMR senses the earth's microwave emission at four frequencies (6.6, 10.65, 18 and 21 GHz), each with vertical (V) and horizontal (H) polarizations. The scanning is conical with a constant incidence angle of 49.7°. The received signal is digitized with 12-bit precision[6]. The MSMR payload has a swath of 1350 km and collects global data with a repeativity of 2 days. The data are recorded on an on-board tape recorder and downloaded during a pass over Hyderabad ground station in India. Digital files of geolocated and calibrated brightness temperature ($T_b$) values are generated from the above measurements. Compared to the currently operating SSM/I, MSMR has additional low frequency channels (6.6-V, 6.6-H, 10.65-V, 10.65-H and 21-H) which, in combination with other MSMR channels, provide an opportunity for development of new applications relating to Antarctic studies. It may also be mentioned that in Nimbus-7 SMMR, the 21 GHz channels were unusable due to excessive noise[7].

We have analysed MSMR weekly averaged brightness temperature ($T_b$) data covering the Antarctic and southern polar region (50°–90°S) for the period June to October 1999. MSMR observed brightness temperatures have been mapped onto a polar-stereographic projection in order to have a clear portrayal of the Antarctic region.

The $T_b$ maps of Antarctica are prepared for 18 and 21 GHz frequencies corresponding to both V and H polarizations. These frequencies are selected because of their higher spatial resolution (50 km × 50 km) compared to the two lower frequency channels. In polar regions, the contribution from the atmosphere is low, in the absence of storms, for the MSMR frequency range[2]. Therefore, the $T_b$ maps at 18 and 21 GHz are largely free of atmospheric contribution and represent the surface conditions reasonably well. The MSMR data acquired over the Antarctic region show several important features related to both the land and the sea. The 21 GHz channel is more responsive to the atmospheric water vapour contribution and this is reflected in the form of relatively warm patches over the open water areas near the northern extremities of the southern ocean. However, over the Antarctic region, this contribution is further reduced due to low atmospheric and surface temperatures. Figure 1 *a* shows the weekly averaged $T_b$ map at 21 GHz (V) for the period 1–7 July 1999. Figure 1 *b* and *c* shows similar $T_b$ maps for the periods 1–7 August 1999 and 26–30 October 1999, respectively.

Over the oceanic region surrounding the Antarctic continent, the observed $T_b$ of open water is low due to its low emissivity (0.28–0.62 in the frequency range 6.6–21 GHz). This is represented by blue and greenish blue colour in Figure 1. $T_b$ values show an increasing trend over ice-covered waters due to higher emissivity of ice. Due to varying degree of the percentage composition of ice and water within a resolution cell, different concentrations of ice show up as having different $T_b$. These are represented by different shades of colours, ranging from yellow to pink. A clear demarcation between open water and sea-ice, all around the Antarctic continent, can be easily seen. Also, on comparing Figure 1 *a* and *b*, it is seen that the ice boundary has expanded in August compared to that in July. Further, during October we find a bigger ice-covered region than in August. The $T_b$ range over ice-covered area is as large as 200–250 K, allowing separation of many categories of sea-ice concentrations.

Over the land mass of Antarctica, very low $T_b$ values (approaching 150 K) are observed over the high plateaus, in spite of the high emissivity of ice (0.62–0.96) in the frequency range 6.6 to 21 GHz (ref. 2). This is

*a*

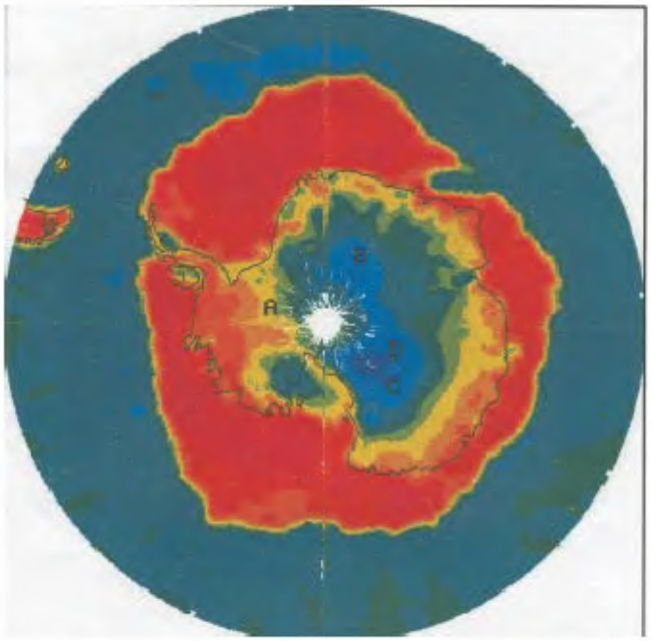


*b*

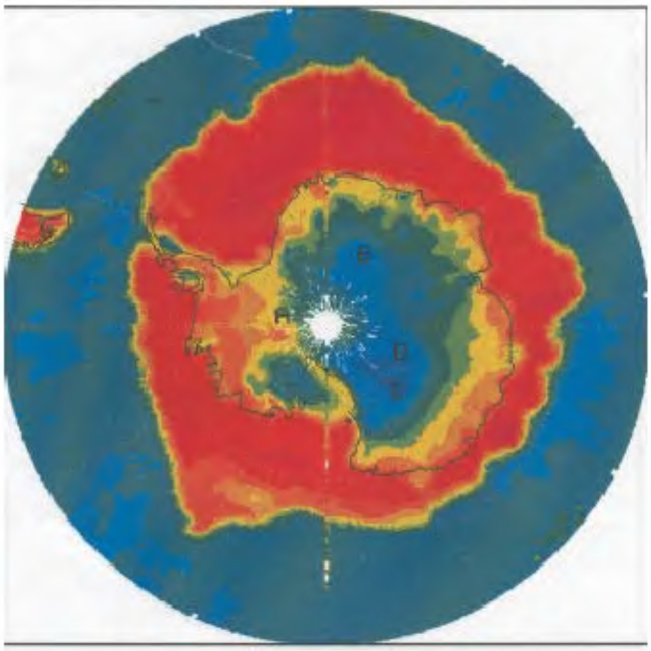


**Figure 1.** Weekly average brightness temperature image over antarctic region (50°–90°S) at 21 GHz (V) from IRS P4-MSMR during (*a*) 1–7 July 1999; (*b*) 1–7 August 1999. A, Trans Antarctic mountain ranges; B, Gamburtsev sub-glacial mountain; C, Wilkes sub-glacial basin; D, Aurora sub-glacial basin.

*c*

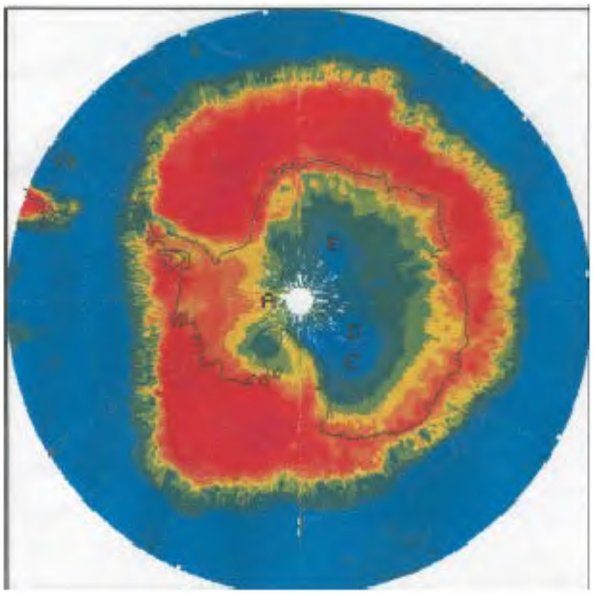


**Figure 1.** *c*, Weekly average brightness temperature image over antarctic region (50°–90°S) at 21 GHz (V) from IRS P4-MSMR during 26–30 October 1999. A, Trans Antarctic mountain ranges; B, Gamburtsev sub-glacial mountain; C, Wilkes sub-glacial basin; D, Aurora sub-glacial basin.

because most parts of Antarctica, except the coastal regions, are covered by mountains and plateaus with elevations ranging from 2 to 4 km. Therefore, very low physical temperatures prevail at higher altitudes, resulting in low $T_b$ represented by the violet, blue and green colours in Figure 1. It may also be mentioned that at higher elevations ice is likely to be older, and the emissivity of old ice being lower, may also contribute to lowering of brightness temperatures. The slope of the mountain ridges also plays an important role in determining the emitted radiation from the ground. As one comes down the slopes, $T_b$ increases and is seen as change of colour from green to yellow to brown. This is because of increase in physical temperature with decreasing altitude according to the dry adiabatic lapse rate.

Many features of land-ice can be inferred from the average $T_b$ maps presented in Figure 1. For example, the well known Trans-Antarctic mountain ranges (A in Figure 1 *a*) and regions of high glacial activity along the east Antarctic coast. In addition to the above, some new features have also been captured by MSMR images, which correspond well to the well-defined geological features of Antarctica, namely part of Gamburtsev sub-glacial mountain (B in Figure 1 *a*), Wilkes sub-glacial basin (C in Figure 1 *a*) and Aurora sub-glacial basin

(D in Figure 1 *a*). It is interesting to note that some of the features, which are reflected very well in the $T_b$ maps of July and August are not seen so well in the $T_b$ map for the last week of October (Figure 1 *c*). This could be attributed to the fact that the contrast in the $T_b$ between two different elevations reduces with the increasing physical temperatures in Antarctica due to the onset of summer in the month of October.

The above study demonstrates the capability of MSMR on-board OCEANSAT-1 in capturing the sea-ice distribution over the Antarctic Circumpolar Sea, as well as the land-ice signatures matching with some known geomorphological features on the continent of Antarctica, thus giving confidence in using MSMR data for studies of earth's polar regions. Quantitative estimation of sea-ice concentration and studies of sea-ice distribution and dynamics are being attempted separately with the help of multi-channel MSMR observations and will be reported soon. Availability of 6.6/10.65 GHz channels on MSMR, not existing on SSM/I, in Antarctic ice studies is also being explored.

1. Gloersen, P., Nordberg, W., Schmugge, T. J., Wilheit, T. T. and Campbell, W. J., *J. Geophys. Res.*, 1973, **78**, 3564–3572.
2. Gloersen, P., Campbell, W. J., Cavalier, D. J., Comiso, J. C., Parkinson, C. L. and Zwally, H. J., Report, NASA SP–511, 1992, pp. 1–290.
3. Steffen, K. and Schweiger, A., *J. Geophys. Res.*, 1991, **96**, 21971–21987.
4. Majumdar, T. J. and Mohanty, K. K., *Curr. Sci.*, 2000, **79**, 648–651.
5. Brigham, A. W. and Drinkwater, M. R., *IEEE GS&RS*, 2000, **38**, 1810–1816.
6. Report, Indian Space Research Organization, 1999, pp. 1–7.
7. Fu, C. C., Han, D., Kim, S. T. and Gloersen, P., Report, NASA RP-1210, 1988, p. 158.

ACKNOWLEDGEMENTS. We wish to acknowledge the encouragement given by Dr R. R. Navalgund and Dr M. S. Narayanan during the course of this work. Useful discussions with Dr P. S. Desai and Dr A. Sarkar are also thankfully acknowledged.

Received 28 July 2000; revised accepted 3 January 2001

# An occurrence of ~ 74 ka Youngest Toba Tephra from the Western Continental Margin of India

**J. N. Pattan[†,*], P. Shane[#], N. J. G. Pearce[‡], V. K. Banakar[†] and G. Parthiban[†]**

[†]National Institute of Oceanography, Dona Paula, Goa 403 004, India
[#]Department of Geology, University of Auckland, P.B. 92019, Auckland, New Zealand
[‡]Institute of Geography and Earth Sciences, University of Wales, Aberystwyth, SY23 3DB, UK

**A dispersed volcanic ash layer was recovered at ~ 300 cm depth in a 5.52 m long sediment core collected at a latitude 9°21′N and longitude 71°59′E from a water depth of 2300 m on the Western Continental Margin of India (WCMI). Glass shards from ash layer were studied for morphology, major, trace and rare earth element concentration to trace the source. Bubble wall junction-type morphology of glass shard suggests magmatic origin. Shards have high $SiO_2$ (77%) and total alkalis (8.5%), indicating rhyolitic composition. The major, trace and rare earth element composition of these glass shards are indistinguishable from that of Youngest Toba ash of ~ 74 ka from the Northern Sumatra and confirm as the source. The new occurrence of Youngest Toba Tuff from the WCMI, Central Indian Ocean Basin and South China Sea Basin suggests a reassessment of the ash volume and global climatic implications.**

VOLCANIC ash in marine sediments is derived either from the continent through wind and river runoff or from *in situ* submarine volcanism. Ash layers of variable thickness in the Bay of Bengal, north-eastern Indian Ocean, Indian subcontinent and Central Indian Ocean Basin were noticed and were attributed to different sources[1–10]. During International Indian Ocean Expedition (1960–1965), a number of sediment cores were retrieved along the Western Continental Margin of India (WCMI). Some sediment cores contained dispersed volcanic glass shards at subsurface depths, but their origin could not be traced[11]. Recently, we have recovered a dispersed ash layer ~ 34 cm thick (324–290 cm depth) in one of the cores collected from the WCMI. The present study is made on this ash to trace the source.

A 5.52 m long sediment core was raised from a water depth of 2300 m at a latitude 9°21′N and longitude 71°59′E from the WCMI in the Arabian Sea, using a gravity corer during ORV *Sagar Kanya* cruise 129 (Figure 1). The core was subsampled at 2 cm intervals onboard and in the laboratory sediment was made salt-free and the coarse fraction (> 63 μm) was obtained by wet sieving. Abundant volcanic glass shards were found between 324 and 290 cm interval of the coarse fraction. The glass shards were separated using heavy liquid bromoform and cleaned ultrasonically. Morphology of glass shards was studied using scanning electron microscopy (JSM-5800LV). Purified glass shards were mounted in epoxy resin and polished to expose internal features. Major element oxides were analysed using Jeol JXA-5A electron microprobe fitted with a Link Systems LZ-5 EDS detector with an absorbed current of 0.5 nA at 15 kV and a beam focused at 10 μm. Thirteen trace and fourteen naturally occurring rare earth elements (REE) were determined for these glass shards using a VG Elemental Plasma Quad II + Inductively Coupled Plasma-Mass Spectrometry (ICP-MS)

*For correspondence. (e-mail: pattan@csnio.ren.nic.in)